

Diffusion-controlled growth of a solid cylinder into its undercooled melt: Instabilities and pattern formation studied with the phase-field model

M. Conti, F. Marinozzi, and U. Marini Bettolo Marconi

Dipartimento di Matematica e Fisica, Universita' di Camerino, 62032 Camerino, Italy

(Received 24 May 1996)

Instabilities in the solidification of a cylinder in its undercooled melt are numerically studied within the phase-field model. This growth becomes morphologically unstable when its radius exceeds a critical value R^* , that is a decreasing function of the thermodynamic driving force: the circular growth regime should be hardly observable, in practice, except possibly at extremely low values of the dimensionless undercooling Δ . However, the equation for the amplitude of the perturbing modes shows that the response of the growing front to a finite noise is drastically reduced when Δ is increased, so that a more stable growth should be associated to larger undercoolings. This suggestion is confirmed by the numerical simulations, which allow us to fix the onset and the extent of the perturbations. To summarize the results, an effective critical radius is represented as a function of Δ . [S1063-651X(97)13902-2]

PACS number(s): 05.70.Fh, 68.70.+w, 61.50.Ks

I. INTRODUCTION

Pattern formation during nonequilibrium growth has been addressed in several studies; extensive reviews are given in [1–3]. Particular attention has been focused on first-order phase-transition processes, in which at least one conserved quantity (heat of solidification or solute material) has to be rejected away from the advancing front. Starting from the seminal papers of Mullins and Sekerka [4,5], the central role in the selection of growth patterns has been recognized in the interplay between the macroscopic thermodynamic driving force (undercooling or supersaturation) and the microscopic interfacial dynamics, that sets the proper length scale, i.e., the capillary length d_0 , necessary for the pattern description. While a linear analysis allows us to identify the spectrum of the unstable modes (at least under some simplifying assumptions), little attention has been paid to the detailed description of the growth process at the early stage, when the frequency spectrum of the fluctuations enters the instability band and the unperturbed front is rapidly destroyed.

For the steady growth of a needle crystal, this subject has been recently addressed by Brener *et al.* [6] within a free-boundary numerical approach. They show that the dendrite tip starts to deform when the amplitude of the perturbations exceeds a threshold value that is dependent on the anisotropy of the surface tension; small amplitude fluctuations are convected away and disappear from the tip region.

Another situation of interest is that of a solid particle nucleated in its undercooled melt. As the action of the surface tension is directed to minimize the surface to volume ratio, at first the shape selected is circular (in two dimensions) or spherical (in three dimensions). No steady solutions can be found in these geometries, because the rate of growth of the particle depends upon its radius, which is increasing with time. In both cases a linear stability analysis performed within the quasistationary approximation shows that the germ becomes morphologically unstable when its radius exceeds a critical value R^* , that is a decreasing function of the undercooling Δ : only at very low values of Δ should the symmetrical growth be practically observable.

However, the onset and the development of perturbations

on the growing front in response to a finite noise has not yet been investigated. In the present study this point will be addressed both analytically, within the free-boundary picture, and numerically, simulating the growth process with the phase-field model [7,8]. To render tractable the numerical approach, the analysis will be limited to the two dimensional (2D) case (cylindrical or circular growth), still retaining some of the most interesting features of the full three dimensional (3D) problem.

The analysis of the governing equation will show that the amplitude of the perturbing modes, in the early stage of the process, is drastically reduced when Δ is increased, so that a more stable growth should be associated to larger undercoolings.

We consider a pure substance, so that the diffusion field is given by the dimensionless temperature $u(x,t) = c[T(x,t) - T_m]/L$, while the driving force is the undercooling $\Delta = c(T_m - T_0)/L$, where T_m and T_0 represent the coexistence temperature of the two phases and the initial temperature of the melt, respectively; c and L are the specific and latent heat per unit volume.

The phase-field approach removes the necessity of tracking the front position, that is found as a part of the numerical solution, and incorporates in a natural fashion both surface tension and surface kinetics effects. On the other hand, the classical free-boundary formulation of the problem is recovered asymptotically when the solid-liquid interface is sufficiently sharp [9].

The model gives a diffuse interface picture of the solidification process, and besides the capillary length introduces a new length scale, that is the interface thickness δ . Realistic values of this parameter fall in the range of several atomic dimensions [10]. In 2D numerical simulations, the grid spacing must be selected in the order of δ while, to prevent finite size effects, the dimensions of the computational domain must be much larger than the thermal diffusion length. As a result, the cost of the solution increases as δ^{-4} , and even simple problems would result beyond the possibilities of the present day computing resources. In this study, following a suggestion of Wheeler, Boettinger, and McFadden [11], a value is selected for the interface thickness that is small com-

pared to the lowest geometric scale that characterizes the process, namely, the local radius of curvature of the perturbed front, and, nevertheless, more than ten times greater than realistic values.

The paper is organized as follows: in Sec. II a linear stability analysis of the free boundary equations will be conducted, to find the dependence of the critical radius R^* on the undercooling Δ ; then the solution of the amplitude equation for the perturbing modes will show that lower perturbations correspond to larger values of Δ . In Sec. III the phase-field model will be introduced, along with the method utilized to obtain the numerical solution. In Sec. IV the results of the simulations will be presented, and Sec. V will give some conclusions.

II. STABILITY OF THE CIRCULAR GROWTH: AMPLITUDE OF THE PERTURBING MODES

The onset of instabilities in the growth of a solid cylinder into its undercooled melt is easily shown through a linear analysis of the free-boundary equations. For this purpose, the system considered is a solid cylinder with radius R surrounded by undercooled liquid in a cylindrical container with fixed temperature $u = -\Delta$ at the wall. The radius of the container is R_c . The rate of growth is limited by the diffusion of latent heat away from the interface; the dynamical field is then the local temperature, that obeys the diffusion equation

$$u_t = \nabla^2 u. \quad (1)$$

Here, and in the following, the problem is treated in dimensionless form, using some reference length ξ , and with time scaled to ξ^2/D . Neglecting the departure from thermodynamical equilibrium, the diffusion field u must fulfill the interface condition

$$u_{\text{int}} = -d_0 \mathcal{K}. \quad (2)$$

The capillary length d_0 is defined as $d_0 = (cT_m/L)(\sigma/L)$, where σ is the surface tension, and \mathcal{K} is the local curvature of the interface. The energy conservation at the interface relates the temperature gradients on the liquid and solid sides of the front to its normal velocity v_n

$$v_n = -[\nabla u_l - \nabla u_s]_{\text{int}} \cdot \mathbf{n}, \quad (3)$$

where \mathbf{n} is the normal versor to the interface. The problem gives a simple solution in the quasistationary approximation, (instantaneous response of the thermal field to the actual front configuration). In this limit, valid for small undercoolings, Eq. (1) reduces to the Laplace equation. Its circular symmetric solution is

$$u(r) = -d_0 \mathcal{K} + \frac{d_0 \mathcal{K} - \Delta}{\ln(R_c/R)} \ln(r/R), \quad r > R \quad (4)$$

$$u(r) = -d_0 \mathcal{K}, \quad r \leq R \quad (5)$$

and the interface velocity is

$$v = -\frac{d_0 \mathcal{K} - \Delta}{\ln(R_c/R)R}. \quad (6)$$

The stability of the circular solution can be tested assuming a small perturbation on the interface, of the form

$$\delta R = \epsilon_m e^{im\phi + \omega t} \quad (7)$$

that involves variations of the temperature field

$$\delta u_{(l,s)} = \theta_{m(l,s)} e^{im\phi + \omega t}, \quad (8)$$

where the subscripts (l,s) refer to the liquid and solid phases, respectively; ϕ is the angular coordinate, that accounts for the loss of circular symmetry of the interface. Solving the Laplace equation for the perturbation gives, to first order,

$$\theta_{m(s)} = -d_0(m^2 - 1)\epsilon_m R^{-(m+2)} r^m, \quad (9)$$

$$\theta_{m(l)} = \left[v_n - \frac{d_0(m^2 - 1)}{R^2} \right] \epsilon_m R^m r^{-m} \quad (10)$$

and the exponential growth rate is found as

$$\omega_m = \frac{v_n}{R} (m - 1) \left[1 - \frac{2\lambda_0^2 m(m+1)}{R^2} \right], \quad (11)$$

with $\lambda_0 = \sqrt{d_0 l_{th}}$; here l_{th} is the thermal diffusion length, given by $l_{th} = 1/v_n$. Equation (11) states that ω_m is an increasing function of the front velocity v_n , and becomes positive as R increases beyond $R^* = \lambda_0 \sqrt{2m(m+1)}$; for $m=2$ (the most unstable mode) $R^* = 2\sqrt{3}\lambda_0$. It is worth noting that since λ_0 decreases with an increasing front velocity (i.e., the undercooling Δ), the unperturbed circular front could survive after the early stage of the growth only at very low values of Δ .

However, a different perspective is offered when the effect of finite noise on the front stability is investigated. Let us assume that on the interface is a continuously acting noise of the form

$$\eta_m(t) = Q(t) \gamma_m e^{im\phi}, \quad (12)$$

where $\langle Q(t)Q(t') \rangle = \delta(t-t')$, and $\langle Q(t) \rangle = 0$; γ_m is the noise amplitude. The interface evolution of the m mode is described by

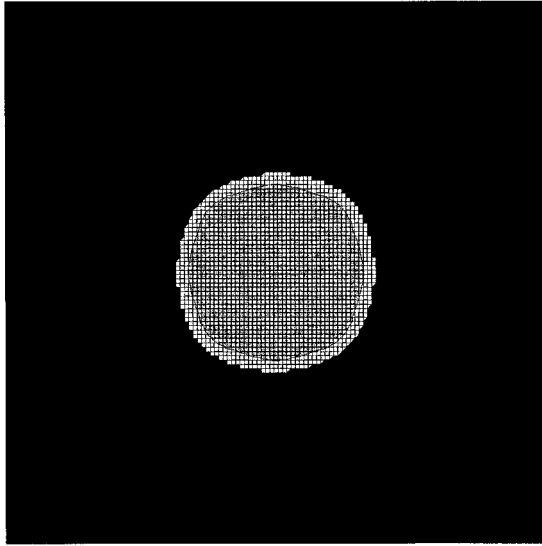
$$\dot{\epsilon}_m = \omega_m \epsilon_m + \eta_m(t). \quad (13)$$

Integrating Eq. (13) gives, for the mode amplitude,

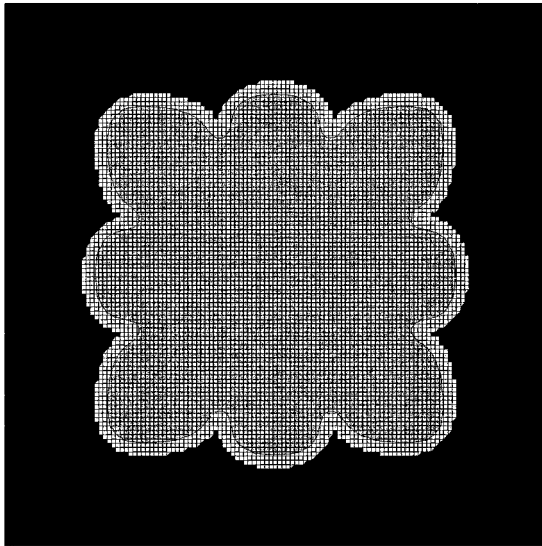
$$\langle |\epsilon_m(t)|^2 \rangle = \langle |\epsilon_m(0)|^2 \rangle e^{2\bar{\omega}t} + \frac{\gamma_m^2}{2\bar{\omega}} (e^{2\bar{\omega}t} - 1), \quad (14)$$

where $\bar{\omega}$ is the time average of ω_m .

The two terms on the right-hand side of Eq. (14) describe two different processes: the evolution of an initially imposed perturbation, and the noise induced perturbation. As $\bar{\omega}$ is of the order of v_n/R , it follows that $\bar{\omega}t$ is of order one; then Eq. (14) suggests that the noise effect would decrease with increasing $\bar{\omega}$, i.e., the front velocity; ultimately increasing the supercooling Δ would result in a damping effect on the front instabilities. In the following sections this suggestion will be confirmed by simulating numerically the growth process with the phase-field model.



(a)



(b)

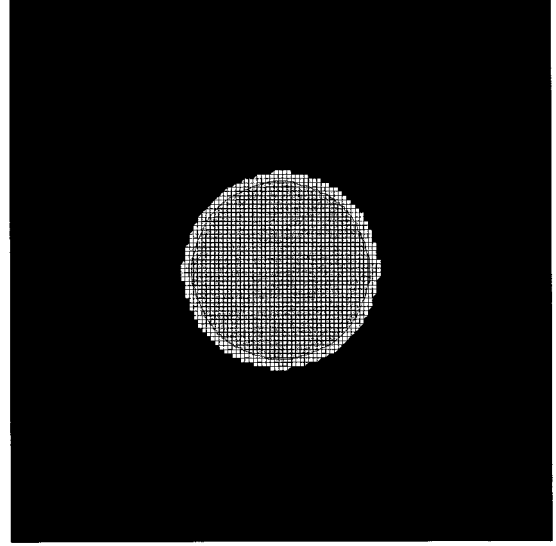
FIG. 1. (a) The solid seed at $t=0.06$. $\Delta=0.6$. (b) The solid seed at $t=0.2$. $\Delta=0.6$.

III. THE PHASE-FIELD MODEL: GOVERNING EQUATIONS AND NUMERICAL TECHNIQUES

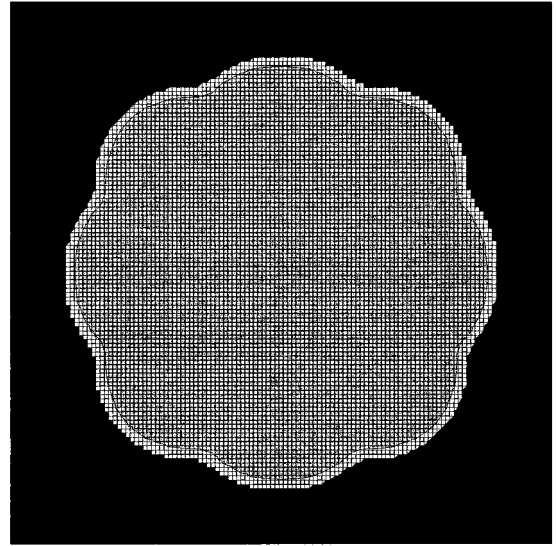
The model describes the solidification of a pure substance in terms of two fields: the scalar phase field $\phi(x,t)$ coupled to the dimensionless temperature field $u(x,t)$. The field ϕ is an order parameter and represents a solid for $\phi=0$ and a liquid for $\phi=1$. Intermediate values correspond to the interface between these two phases. The dynamical equations, derived along the lines suggested by Penrose and Fife [12], and then followed by Wang *et al.* [13], are the following:

$$\frac{\partial u}{\partial t} = \nabla^2 u - p'(\phi) \frac{\partial \phi}{\partial t}, \quad (15)$$

$$\frac{\epsilon^2}{m} \frac{\partial \phi}{\partial t} = \epsilon^2 \nabla^2 \phi + \phi(1-\phi)(\phi - \frac{1}{2}) + \epsilon \alpha p'(\phi) u + \Gamma(t). \quad (16)$$



(a)



(b)

FIG. 2. (a) The solid seed at $t=0.03$. $\Delta=0.9$. (b) The solid seed at $t=0.09$. $\Delta=0.9$.

The function $p(\phi) = \phi^3(10 - 15\phi + 6\phi^2)$ enforces the condition that the kinetic equations have two fixed points at $\phi=0$ and $\phi=1$ for every value of u . $\Gamma(t)$ represents the noise acting on the interface. The three dimensionless constants appearing in Eqs. (15) and (16) were related by Wheeler, Murray, and Schaefer [14] to the material properties, namely, $\alpha = \sqrt{2} \xi L^2 / (12c\sigma T_m)$, $m = \mu\sigma T_m / (DL)$ and $\epsilon = \delta' \xi$, where μ represents the kinetic undercooling coefficient. In the following numerical simulations we put $\alpha=200$, $m=0.05$, and $\epsilon=0.01$; fixing the length scale at $\xi=1.05 \times 10^{-4}$ cm, these values mimic, as close as possible, the thermophysical properties of nickel near its melting temperature [15].

Equations (15) and (16) have been solved on a two dimensional square domain $0 \leq x \leq \lambda$, $0 \leq y \leq \lambda$; fixing $\lambda=7.65$ was sufficient to prevent finite size effects. Adiabatic conditions were imposed on the domain's boundaries. Initially, in the undercooled melt ($u=-\Delta$, $\phi=1$) a solid seed ($u=0$,

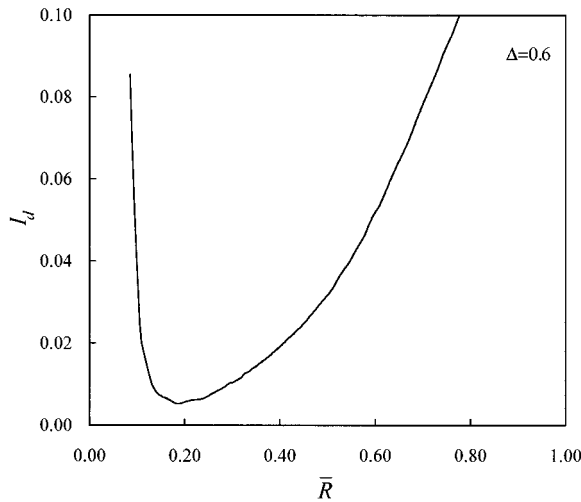


FIG. 3. Distortion index of the circular front vs the average radius of the seed. $\Delta=0.6$.

$\phi=0$) is prepared at the center of the square. The size of the seed (3×3 grid points) is the minimum required to avoid remelting and to ensure the successive growth. To discretize the equations, a uniform spatial grid is utilized, with $\Delta x = \Delta y = 0.01$; the Laplace operator is approximated through a five point formula and an explicit Euler integration scheme is employed to advance forward in time. A time step $\Delta t = 0.2 \times 10^{-4}$ was required to ensure the stability of the numerical scheme. The resolution of the grid was chosen following the suggestion of Wheeler, Murray, and Schaefer [14], to limit the truncation errors of the Laplace operator; the residual contribution of the numerical noise results in a superposition of circular modes acting on the interface, and has been utilized as the noise source $\Gamma(t)$.

IV. NUMERICAL RESULTS

The initially square solid seed grows into the melt; the action of the surface tension is directed as to minimize the surface to volume ratio, and very soon the interface becomes almost circular. Then, as the radius of the seed exceeds R^*

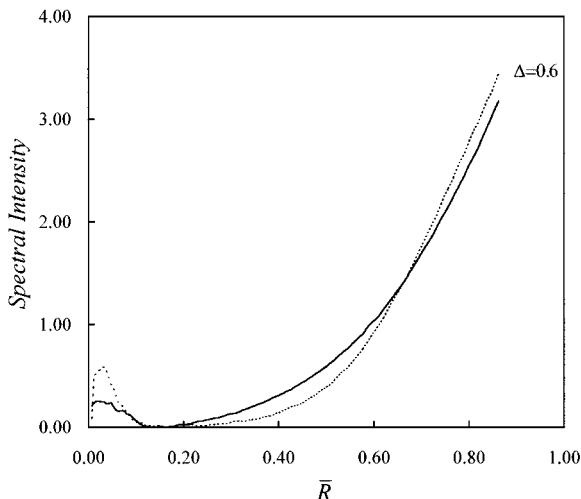


FIG. 4. Spectral intensities of the modes $m=4$ (solid line) and $m=8$ (dotted line), vs the average radius of the seed. $\Delta=0.6$.

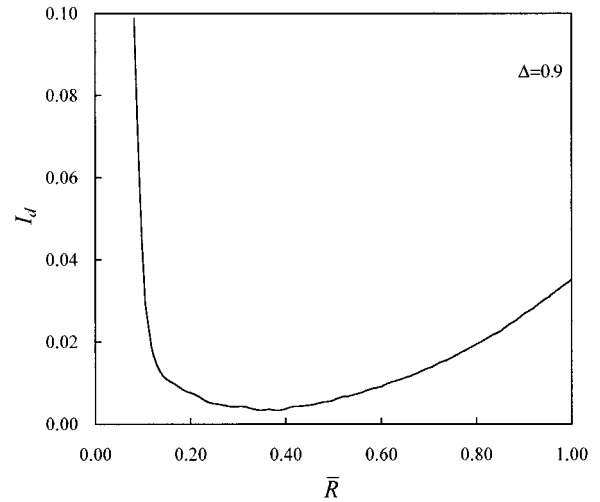


FIG. 5. Distortion index of the circular front vs the average radius of the seed. $\Delta=0.9$.

the perturbations start to grow. A typical example of such behavior is given in Figs. 1(a) and 1(b), where the growing solid is shown at two different times. Here the undercooling is $\Delta=0.6$. Changing the undercooling has a strong effect on the deformation of the interface. Figures 2(a) and 2(b) show the solid seed at two different times, with $\Delta=0.9$; it can be observed that here the extent of the deformations is considerably lower.

To describe the extent of the deformation a distortion index is defined as

$$I_d = \frac{1}{\bar{R}(\phi)} \sqrt{R^2(\phi) - \bar{R}(\phi)^2}. \quad (17)$$

The function $R(\phi)$ is evaluated dividing the computational domain into 64 circular sectors of equal width $\Delta\phi = 2\pi/64$, centered at the initial position of the seed. In each sector the front position is fixed through the relation

$$\frac{1}{2}R^2(\phi)\Delta\phi = S(\phi), \quad (18)$$

where $S(\phi)$ is the solid area in the sector considered.

The distortion I_d is evaluated, during the evolution of the process, at regular intervals of time; moreover, a Fourier analysis is performed with the same periodicity on the function $R(\phi)$, in order to identify the presence and the growth of the perturbing modes.

Figure 3 shows the distortion I_d versus \bar{R} for $\Delta=0.6$. It can be observed that I_d is high at the beginning of the process, due to the square shape of the initial nucleus. Then the initial distortion is rapidly reabsorbed, and I_d reaches a minimum at $\bar{R}=0.18$, where the distortion is less than 0.01; beyond this value the onset of the perturbations is clearly recognizable. These results are complemented by Fig. 4, where the spectral intensities of the two circular harmonics $m=4$ and $m=8$ are represented versus \bar{R} . At first, as ω_4 becomes positive, the mode $m=4$ greatly increases; successively the mode $m=8$ enters the instability band and starts to grow. The crossover of the two curves at $\bar{R}=0.65$ indicates that at a later stage of the growth the propagation of the mode $m=8$ is

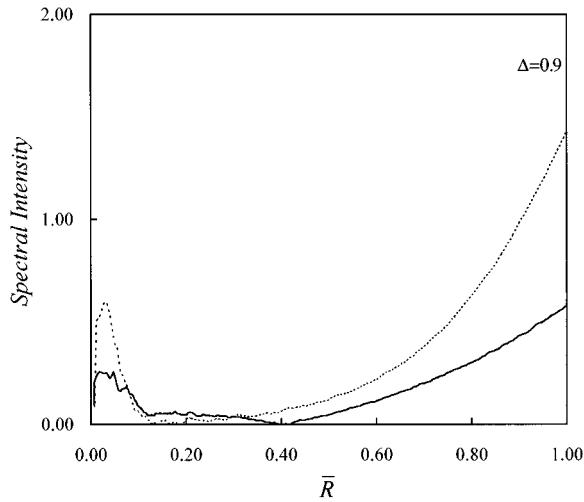


FIG. 6. Spectral intensities of the modes $m=4$ (solid line) and $m=8$ (dotted line), vs the average radius of the seed. $\Delta=0.9$.

avored; however, this behavior cannot be amended to a straightforward analysis of Eq. (14).

Figure 5 gives the same informations than Fig. 3, but now $\Delta=0.9$. In this case too the initial distortion is substantially reabsorbed when $\bar{R} \leq 0.1$, but here the onset of the perturbations is retarded, and I_d reaches its minimum at $\bar{R}=0.35$ where the distortion is less than 0.005; at $\bar{R}=0.5$ I_d is still below 0.01. Figure 6 shows that now the intensity of the mode $m=4$ at the early stage is strongly damped, due to the low prefactor $1/\bar{\omega}$ in Eq. (14); beyond $\bar{R}=0.3$ the mode $m=8$ is prevailing.

The value of \bar{R} where the minimum of I_d occurs, can be regarded as an effective critical radius $R^{*'}$ for the stability of the circular growth; Fig. 7 shows that $R^{*'}$ increases with increasing the supercooling Δ , indicating that the symmetry of the circular front is more easily preserved at large values of Δ .

V. CONCLUSIONS

The growth of a cylinder of solid into the undercooled melt has been analyzed in two dimensions. The circular front

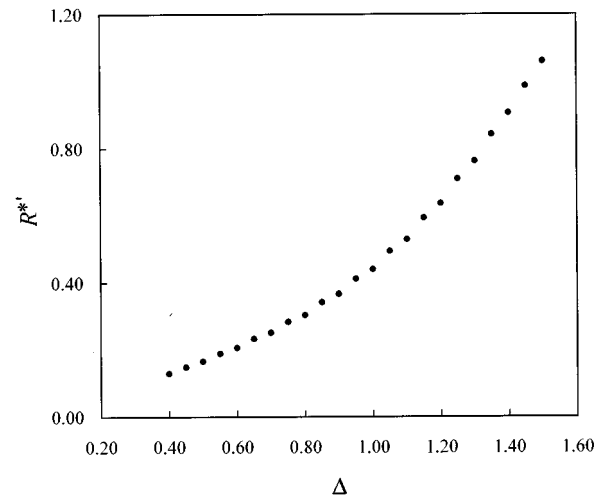


FIG. 7. The effective critical radius of the circular front vs the supercooling Δ .

becomes unstable beyond a critical size and is rapidly destroyed. According to the stability analysis of the free-boundary equations, the onset of the perturbations is expected to occur at lower values of the cylinder radius as the undercooling Δ increases; on the other side the amplitude equation for the perturbing modes shows that the extent of the deformations in response to a finite noise should be reduced with increasing Δ . This suggestion is confirmed by a simulation of the process, conducted using the phase-field model. The numerical results show that at large values of Δ the onset of the perturbations is retarded and the circular symmetry of the growing front is effectively preserved at larger values of the cylinder radius.

Due to the limitation of computing resources it is not possible, at present, to conduct the numerical simulation in three dimensions, to describe the onset and the development of perturbations in the growth of a spherical germ. Nevertheless, the 2D problem still retains some of the most interesting features that characterize the spherical growth, and the results we presented should provide a satisfactory insight even of the three dimensional case.

-
- [1] J. S. Langer, *Rev. Mod. Phys.* **52**, 1 (1980).
 [2] D. A. Kessler, J. Koplik, and H. Levine, *Adv. Phys.* **37**, 225 (1988).
 [3] E. A. Brener and V. I. Mel'nikov, *Adv. Phys.* **40**, 53 (1991).
 [4] W. W. Mullins and R. F. Sekerka, *J. Appl. Phys.* **34**, 323 (1963).
 [5] W. W. Mullins and R. F. Sekerka, *J. Appl. Phys.* **35**, 444 (1964).
 [6] E. Brener, T. Ihle, H. Muller-Krumbhaar, Y. Saito, and K. Shiraiishi, *Physica A* **204**, 96 (1994).
 [7] J. S. Langer, in *Directions in Condensed Matter Physics*, edited by G. Grinstein and G. Mazenko (World Scientific, Singapore, 1986).
 [8] G. Caginalp, in *Applications of Field Theory to Statistical Mechanics*, edited by L. Garrido (Springer-Verlag, Berlin, 1984).
 [9] G. Caginalp, *Phys. Rev. A* **39**, 5887 (1989).
 [10] D. W. Oxtoby and D. J. Haymet, *J. Chem. Phys.* **76**, 6262 (1982).
 [11] A. A. Wheeler, W. J. Boettinger, and G. B. McFadden, *Phys. Rev. A* **45**, 7424 (1992).
 [12] O. Penrose and P. C. Fife, *Physica D* **43**, 44 (1990).
 [13] S. L. Wang, R. F. Sekerka, A. A. Wheeler, B. T. Murray, S. R. Coriell, R. J. Braun, and G. B. McFadden, *Physica D* **69**, 189 (1993).
 [14] A. A. Wheeler, B. T. Murray, and R. J. Schaefer, *Physica D* **66**, 243 (1993).
 [15] F. Marinuzzi, M. Conti, and U. Marini Bettolo Marconi, *Phys. Rev. E* **53**, 5039 (1996).